

LECTURE 10

Gravitational waves from neutron stars

S. Bonazzola and E. Gourgoulhon

Département d'Astrophysique Relativiste et de Cosmologie,
 UPR 176 C.N.R.S.,
 Observatoire de Paris,
 F-92195 Meudon Cedex, France

1. INTRODUCTION

A crude estimate of the gravitational luminosity of an object of mass M , mean radius R and internal velocities of order V can be derived from the quadrupole formula [1]:

$$L \sim \frac{c^5}{G} s^2 \left(\frac{R_s}{R} \right)^2 \left(\frac{V}{c} \right)^6, \quad (1)$$

where $R_s := 2GM/c^2$ is the Schwarzschild radius associated with the mass M and s is some asymmetry factor: $s = 0$ for a spherically symmetric object and $s \sim 1$ for an object whose shape is far from that of a sphere. According to formula (1), the astrophysical objects for which $s \sim 1$, $R \sim R_s$ and $V \sim c$ may radiate a fantastic power in the form of gravitational waves: $L \sim c^5/G = 3.6 \times 10^{52}$ W, which amounts to 10^{26} times the luminosity of the Sun in the electromagnetic domain!

A neutron star has a radius quite close to its Schwarzschild radius: $R \sim 1.5 - 3 R_s$ and its rotation velocity may reach $V \sim c/2$ at the equator, so that they are a priori valuable candidates for strong gravitational emission. The crucial parameter to be investigated is the asymmetry factor s . It is well known that a uniformly rotating body, perfectly symmetric with respect to its rotation axis does not emit any gravitational wave ($s = 0$). Thus in order to radiate gravitationally a neutron star must deviate from axisymmetry. P. Haensel's

lecture [2] investigates the deviation from axisymmetry resulting from irregularities (“mountains”) in the solid crust or from the neutron star precession. In the present lecture, we investigate two other mechanisms which generate a deviation from axisymmetry: (i) the spontaneous symmetry breaking resulting from the development of a triaxial instability in a rapidly rotating neutron star (§ 2) and (ii) the distortion induced by the internal magnetic field of the neutron star (§ 3).

2. SPONTANEOUS SYMMETRY BREAKING

A rotating neutron star can spontaneously break its axial symmetry if the ratio of the rotational kinetic energy T to the absolute value of the gravitational potential energy, $|W|$, exceeds some critical value. This may occur in two different astrophysical situations: a just born neutron star resulting from a supernova may accrete matter that has not been ejected by the shock wave, thereby increasing its kinetic energy; alternatively, an old neutron star in a close binary system, accreting matter steadily from its companion, may be spun up until the ratio $T/|W|$ is high enough to allow the symmetry breaking.

When the critical threshold $T/|W|$ is reached, two kinds of instabilities may drive the star into the non-axisymmetric state:

1. the *Chandrasekhar-Friedman-Schutz instability* (hereafter *CFS instability*) [3], [4], [5] driven by the gravitational radiation reaction.
2. the viscosity driven instability [6].

The present lecture puts the accent on the viscosity driven instability.

2.1. Review of classical results about Maclaurin/Jacobi ellipsoids

Let us recall some classical results from the theory of rotating Newtonian homogeneous bodies. It is well known that a self-gravitating incompressible fluid rotating rigidly at some moderate velocity takes the shape of an axisymmetric ellipsoid: the so-called *Maclaurin spheroid*. At the critical point $T/|W| = 0.1375$ in the Maclaurin sequence, two families of triaxial ellipsoids branch off: the *Jacobi ellipsoids* and the *Dedekind ellipsoids*. The former are triaxial ellipsoids rotating rigidly about their smallest axis in an inertial frame, whereas the latter have a fixed triaxial figure in an inertial frame, with some internal fluid circulation at constant vorticity (see ref. [7] or [8] for a review of these classical results). The Maclaurin spheroids are dynamically unstable for $T/|W| \geq 0.2738$. Thus the Jacobi/Dedekind bifurcation point $T/|W| = 0.1375$ is dynamically stable. However, in presence of some dissipative mechanism such as viscosity or gravitational radiation (CFS instability) that breaks the circulation or angular momentum conservation, the bifurcation point becomes secularly unstable against the $l = 2, m = 2$ “bar” mode. Note also that a

non-dissipative mechanism such as the one due to a magnetic field with a component parallel to the rotation axis breaks the circulation conservation [9] and may generate a spontaneous symmetry breaking. If one takes into account only the viscosity, the growth of the bar mode leads to the deformation of the Maclaurin spheroid along a sequence of figures close to some Riemann S ellipsoids⁽¹⁾ and whose final state is a Jacobi ellipsoid [11]. On the opposite, if the gravitational radiation reaction is taken into account but not the viscosity, the Maclaurin spheroid evolves close to another Riemann S sequence towards a Dedekind ellipsoid [12].

As we shall see in the next section, this symmetry breaking is a particular case of a more general phenomenon .

2.2. Spontaneous breaking of symmetry: a general phenomenon

2.2.1. A toy model

Let us start with a simple example. Consider the toy model of Fig. 1 : two heavy points of mass m , rigidly connected and sliding on a circular guide of radius R , of negligible mass and rotating with the angular velocity Ω . It is straightforward to write down the expression for the potential energy of this system and to find the equilibrium configuration in a frame rotating with the guide. With the notations of Fig. 1, the potential (potential energy per unit mass) writes:

$$U(\theta) = -(R\Omega)^2(\sin^2 \alpha + \cos 2\alpha \sin^2 \theta) - 2gR \cos \alpha \cos \theta , \quad (2)$$

g being the gravity acceleration. In spite of the invariance of the potential U with respect the transformation $\theta \mapsto -\theta$, two equilibrium configurations exist if the angular velocity is larger than the value $\Omega_{\text{crit}} = [g \cos \alpha / (R \cos 2\alpha)]^{1/2}$: $\theta = 0$ and $\cos \theta = g \cos \alpha / (R\Omega^2 \cos 2\alpha)$.

This behaviour is typical of the phenomenon of spontaneous symmetry breaking. More generally, a dynamical system is said to break spontaneously its symmetry if there exist solutions with lower symmetries than those of the Lagrangian from which the equations of motion have been derived. Other examples of spontaneous symmetry breaking are the phase transitions (ferromagnetism at the Curie point, melting of solids), the famous walking stick in Charlie Chapling movies (the stick is axially symmetric but when the pressure of the hand on its top is larger than a critical value, the stick bends), the buckling collapse of metallic structures and so on.

Coming back to the toy model, it is easy to see that, when two equilibrium configurations exist, the one is unstable and the other one is stable. For what

(¹) The *Riemann S* family is formed by homogeneous bodies whose fluid motion can be decomposed into a rigid rotation about a principal axis and a uniform circulation whose vorticity is parallel to the rotation vector. Maclaurin, Jacobi and Dedekind ellipsoids are all special cases of Riemann S ellipsoids (for more details, cf. Chap. 7 of ref. [7] or Sect. 5 of ref. [10]).

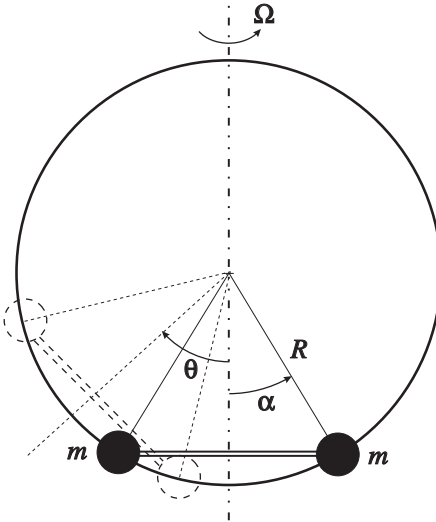


Fig. 1. — Toy model illustrating the phenomenon of spontaneous symmetry breaking: the configuration depicted with dashed lines violates the symmetry with respect to the rotation axis and is a stable equilibrium configuration if $\Omega > \Omega_{\text{crit}}$.

follows it is more convenient to take the angular momentum as a free parameter instead of the angular velocity. Let us suppose that some viscous force acts on the two mass points sliding on the circular guide. If at time $t = 0$, the system is in the equilibrium configuration $\theta = 0$ and its angular momentum L is larger than the critical value L_{crit} corresponding to Ω_{crit} , then the system will move to the second equilibrium configuration. In this example, we have all the main ingredients of the spontaneous symmetry breaking mechanism: a parameter describing the equilibrium configuration of the system, a dynamical quantity that is not conserved (the kinetic energy) and a total energy that must be at its minimum. In order to understand the existence of two equilibrium configurations, it is worth writing the total energy (per unit mass) with respect to the inertial frame in terms of the angular momentum L : $E = 1/2 L^2/I + U_{\text{grav}}$, where $I(\theta)$ is the moment of inertia of the system with respect to the rotation axis and U_{grav} is the gravitational potential: $U_{\text{grav}} = -2gR \cos \alpha \cos \theta$. It is clear that, at fixed L , L^2/I decreases when I increases, i.e. when θ increases. On the contrary, U_{grav} is an increasing function of θ . When L is large enough, the first term prevails and E decreases when θ increases.

In order to see the link existing between the symmetry breaking mechanism of the above toy model and the second order phase transition theory, let us briefly recall the Landau theory of these phenomena (see Chap. 14 of [13]). In a second order phase transition, a thermodynamical system makes a continuous transition from a state with a given symmetry to a state with a

lower symmetry. The leading idea in the Landau theory is the expansion of the thermodynamical potential $\Phi(P, T)$ in a series of a parameter η (the *order parameter*) which measures how far the thermodynamical system is from the state of higher symmetry:

$$\Phi(P, T, \eta) = \Phi_0(P, T) + \alpha\eta + A\eta^2 + B\eta^3 + C\eta^4 + \dots \quad (3)$$

From invariance considerations, α must be identically equal to zero, B must also be equal to zero in order to obtain a stable system. On the contrary, C must be positive. A must be larger than zero in the symmetric phase because the system is stable. On the contrary, in the less symmetric phase, values of η different from zero correspond to a stable state. That is possible only if $A < 0$, therefore A must vanish at the critical temperature: $A = a(T - T_c)$. In conclusion we can write:

$$\Phi(P, T, \eta) = \Phi_0(P, T) + a(T - T_c)\eta^2 + C\eta^4. \quad (4)$$

The value of η in the vicinity of T_c is:

$$\eta^2 = a(T_c - T)/(2C). \quad (5)$$

From the expression (4) for the thermodynamical potential all the interesting thermodynamical quantities and their jumps at the critical temperature can be derived.

Coming back to the toy model, consider the total potential (eq. (2)) and expand it as function of θ around the value $\theta = 0$. The result is

$$\begin{aligned} U = & -(R\Omega \sin \alpha)^2 + R(g \cos \alpha - R\Omega^2 \cos 2\alpha) \theta^2 \\ & + R[R\Omega^2 \cos 2\alpha - (g \cos \alpha)/4] \theta^4/3 + O(\theta^6). \end{aligned} \quad (6)$$

It is easy to see the analogy between expressions (4) and (6). In fact θ is the order parameter of the toy model: when $\theta = 0$ the system is axisymmetric and it breaks this symmetry for $\theta > 0$. The potential U is the analogue of the thermodynamical potential Φ . No extra terms with odd power of θ appear, there is a critical value of Ω for which the quadratic terms vanish and, last but not least, the quartic term is positive in the vicinity of Ω_{crit} . It is straightforward to define a “temperature” of the system. Let us put $T = 1/(R\Omega)^2$; then $T_c = \cos 2\alpha/(gR \cos \alpha)$, $a = 2(gR \cos \alpha)^3/\cos^2 2\alpha$ and $C = (gR \cos \alpha)^2/\cos 2\alpha$. The reader can push the analogy further by defining the equivalent “thermodynamical quantities” and compute their discontinuities at the transition point.

An equivalent treatment (but slightly more complicated) can be employed by replacing Ω by the angular momentum L . In this case α must be different from zero, in order to have a finite angular momentum when $\theta = 0$.

2.2.2. The case of rotating stars

The mechanism of axial symmetry breaking for a rotating star is very similar to the mechanism described in the toy model. When the angular momentum L

of the star is larger than a critical value L_c , the symmetry of the star changes in order to increase its moment of inertia I and consequently to decrease its rotational kinetic energy for a given angular momentum L .

In what follows, it is more convenient to parametrize the rotation of the star by the ratio R of the rotational kinetic energy to the potential energy: $R = T/|W|$ instead of the angular momentum L . In fact, the critical value of R_c at which the symmetry is broken depends only on the equation of state (hereafter EOS) of the fluid which constitutes the star. Moreover, in the case of a polytropic EOS, ($P = \alpha n^\gamma$, n and P being the density and the pressure respectively) R_c depends on γ only. As recalled in § 2.1, for an incompressible star $R_c = 0.1375$ (secular instability).

The symmetry breaking process is, of course, more complicated than the one described for the toy model. The number of degrees of freedom of the star is infinite instead of being just one for the toy model, consequently the analogy cannot be pushed further.

In order to understand what follows, the following theorem is needed:

Theorem: Among all the possible angular velocity distributions in a steady state configuration, rigid rotation ($\Omega = \text{const.}$) minimizes the energy of the star (see the problem at the end of this lecture).

We may now understand what happens to an axisymmetric rigidly rotating star when the angular velocity is slightly larger than the critical one. Consider for the moment the case without dissipative mechanisms. Since at constant angular momentum — larger than the critical one — the configuration which minimizes the total energy of the *rigidly* rotating star is a triaxial one, the star tends to break the axial symmetry and starts to deform to evolve to the new equilibrium configuration. In absence of viscosity or any other dissipative mechanisms, the angular momentum of each shell of the star is conserved and the angular velocity is no more uniform. It turns out that this new configuration, slightly non-axisymmetric has a total energy larger than the old one because the rotation is no more rigid (cf. the above theorem). Therefore the star does not evolve in this way and stays in the axisymmetric configuration.

We may say that the conservation of the angular momentum of each shell acts as a potential barrier that inhibits the transition to the non-axisymmetric equilibrium configuration. The situation is completely different when viscosity is present. When the star starts to deform, the viscosity spreads out the angular momentum, so that the rotation becomes rigid and the star can go to the non-axisymmetric equilibrium configuration. It is obvious that the time taken to make the transition depends on the time required to rigidify the motion: the smaller the viscosity, the longer the time to make the transition. For this reason this instability is called *secular*. When the angular momentum is larger than a second critical value $L_{c,\text{dyn}}$ the potential barrier due to the non-rigid rotation can be overcome and the transition toward the new equilibrium configuration is possible. The corresponding critical value of R is $R_{c,\text{dyn}} = 0.2738$ for an

incompressible fluid. This instability is called *dynamical* for it occurs on a dynamical timescale.

The instability described above is at the origin of the transition of the star from a Maclaurin spheroid to a triaxial Jacobi ellipsoid. Since viscosity-driven evolution preserves the angular momentum but not the kinetic energy, the final equilibrium configuration has the same mass, the same angular momentum and rigid rotation. If the total mechanical energy is conserved but the conservation of the angular momentum is violated, then the Maclaurin steady state configuration makes a transition toward the triaxial Dedekind ellipsoid, which is not rigidly rotating.

Actually, there exists many other bifurcation points, all of them being parameterized by a given value of the T/W ratio (pear configuration found by Poincaré, fission bifurcation, etc...)

From what has been said, the analogy between the mechanism of spontaneous symmetry breaking of the toy model and that of the rotating star should have clearly appeared. Consequently, the transition between the Maclaurin and the Jacobi ellipsoids can be studied by using the theory of second order phase transition, as we have done for the toy model. Historically, Bertin and Radicati [14] were the first to recognize in 1976 that the bifurcations in the steady state configurations of rotating homogeneous stars are genuine second order phase transitions. More recently, Christodoulou, Kazanas, Shlosman and Tohline [15] have systematically used this analogy to study the different bifurcations of rotating homogeneous stars and to investigate the possibility of a transition from one steady state configuration to another one. Not only have they found new results but they have also given more insight to the understanding of this mechanism. We highly recommend their articles [15], [16], [17], [18] to the interested reader.

2.3. Previous results for compressible Newtonian stars

The results on Maclaurin spheroids recalled above have been extended to compressible fluids, modeled by a polytropic EOS, by a number of authors. First of all Jeans [19], [20] has shown that a bifurcation point towards triaxial configurations can exist only if the adiabatic index γ is larger than $\gamma_{\text{crit}} \simeq 2.2$. The interpretation is that the EOS must be stiff enough for the bifurcation point to occur at an angular velocity lower than the maximum angular velocity Ω_K for which a stationary solution exists. Ω_K is reached when the centrifugal force exactly balances the gravitational force at the equator of the star, and for this reason is called the *Keplerian velocity*; if the star were forced to rotate at $\Omega > \Omega_K$, it would lose some matter from the equator. By numerical calculations, James [21] has refined Jeans' result to

$$\gamma_{\text{crit}} = 2.238 \quad (\text{James 1964}). \quad (7)$$

As concerns the secular instability in the compressible case, Ipser & Managan [22] have shown that the $m = 2$ Jacobi-like bifurcation point has the same

location along uniformly rotating sequences as the $m = 2$ Dedekind-like point, as in the incompressible case. For $\gamma < \gamma_{\text{crit}}$, the CFS instability still exists for modes $l = m \geq 3$ [23], [24] but not the viscous instability: if the viscosity is important, its effect is always stabilizing by acting against the CFS instability. Lindblom [25] has shown that for a star of $1.5 M_{\odot}$ constructed by means of a $\gamma = 2$ polytropic EOS, the CFS instability is suppressed at temperatures $T < 5 \times 10^6$ K by the shear viscosity and at $T > 10^{10}$ K by the bulk viscosity. These results have been confirmed by Yoshida & Eriguchi [26] (see also Sect. 2 of ref. [27] and references therein). For completeness, let us note that if the neutron star interior is superfluid, the CFS instability is suppressed by the “mutual friction” of its components [28].

Regarding the gravitational wave signal from rotating neutron stars that undergo the above triaxial instabilities, Ipser & Managan [29] have examined the case of polytropic stars with $\gamma = 2.66$ and $\gamma = 3$ which have bifurcated along a triaxial Jacobi-like sequence, under the effect of the viscosity driven instability. Wagoner [30] has computed the gravitational signal from an accreting neutron star — modeled by nearly spherical homogeneous objects — for the five lowest modes of the CFS instability. Recently, Lai & Shapiro [31] have determined the gravitational wave form from newborn neutron stars — modeled as self-similar ellipsoids — undergoing the bar mode $l = m = 2$ of the CFS instability.

2.4. Generation of gravitational waves

It is worth discussing the role played by the two instability mechanisms, CFS and viscosity-driven, in the emission of gravitational waves by a rotating neutron star. Let us consider a just born neutron star (from the core collapse of a massive star) with a kinetic energy T larger than the critical one. For zero viscosity, the star breaks its symmetry via the CFS mechanism. Its fate is a triaxial Dedekind-like ellipsoid. Because the principal axes of this ellipsoid are fixed in an inertial frame the quadrupole moment is constant and the gravitational radiation stops. On the contrary if the viscosity is larger than a critical value [32], the CFS instability is inhibited and the star evolves toward a Jacobi configuration; it loses energy and angular momentum via gravitational radiation until its kinetic energy achieves the critical value T_c . It turns out that this second mechanism is more efficient for gravitational wave generation than the first one. In the intermediate case, the gravitational radiation light curve depends on the ratio between the rising time of the two instabilities. The real life is more complicated: in fact the EOS is far from being a polytropic. Consequently, the conditions for a bar instability depend on the EOS *and* on the mass of the star. Moreover, neutron stars are strongly relativistic objects and post-Newtonian or even post-post-Newtonian approximations are not sufficient to describe their steady states of rotation. A fortiori, the results obtained in the Newtonian theory can hardly be used to predict the gravitational radiation from these objects.

In what follows, we shall try to answer to the following questions:

1. Among all the EOS proposed for nuclear matter, are there some stiff enough to allow the bar instability ?
2. What is the influence of the general relativistic effects on the bar instability ?
3. In the case of a positive answer to the first question, and under the hypothesis that the general relativistic effects do not kill the bar instability, what are the masses of the stars for which the bar instability can develop ?
4. Are these masses compatible with the masses of neutron stars already observed ?

2.5. Finding the equilibrium configurations of a rotating star in the Newtonian regime

In order to show how the Newtonian results can be extended to general relativity, we need to explain how the equilibrium configurations of rotating barotropic stars are computed. Therefore, this section may appear quite technical. The reader not interested in mathematical and technical problems, can skip this section and go directly to section 2.9.2. He should only remember that the exact solution for the motion of a triaxial rotating star in the framework of general relativity does not exist yet, the results presented in the next sections being obtained under adequate approximations.

Consider a steady state star rotating with constant angular velocity Ω about the z axis. In a frame rotating with the same angular velocity and about the same rotation axis, the star will appear static, therefore the problem of finding a steady state configuration becomes a problem of finding a static configuration. Let n , $P(n)$ be the density and the pressure of the fluid respectively. The barotropic EOS $P = P(n)$ is supposed to be known. The equilibrium equations reads

$$1/n \partial P(n)/\partial \rho + \partial U/\partial \rho - \Omega^2 \rho = 0 \quad (8)$$

$$1/n \partial P(n)/\partial z + \partial U/\partial z = 0, \quad (9)$$

where $U(x, y, z)$ is the self-gravitational potential, and $\rho^2 = x^2 + y^2$. By introducing the specific enthalpy of the fluid,

$$H(n) = \int \frac{1}{n} \frac{dP}{dn} dn \quad (10)$$

the system of differential equations (8)-(9) can be integrated immediately to yield

$$H + U - \frac{1}{2} \Omega^2 \rho^2 = \text{const.} \quad (11)$$

Hence once U is known and H is fixed at the centre of the star, H and therefore n can be easily computed at all the points of the star. The surface of the star is defined by $H = 0$.

The potential U must be computed by solving in a consistent way the 2-D Poisson equation

$$\Delta U = 4\pi G n \quad (12)$$

where G is the gravitational constant. The integration of the system of equations (12), (11) and (10) is performed by relaxation: take a trial distribution of matter n , compute the potential U by solving the Poisson equation, compute the corresponding H by means of Eq. (11), inverse the relationship $H(n)$ to obtain the density n and solve the Poisson equation to find a new potential U until convergence is achieved. About 50 iterations are necessary to obtain numerical solutions that differ less than 10^{-12} between two different iterations. In a such a way a 2-D equilibrium configuration is obtained.

Once the equilibrium configuration is found, its stability can be studied. For this purpose we proceed in the following way: instead of stopping the relaxation at the J^{th} iteration say, the procedure is continued altering slightly the gravitational potential at the $(J+1)^{\text{th}}$ iteration: some perturbation $\epsilon r^2 P_2(\cos \theta) \cos(2\phi)$ is added to the axisymmetric potential, where $r^2 = \rho^2 + z^2$, P_2 is the Legendre polynomial of degree 2 and ϵ a numerical constant ($\epsilon = 10^{-6}$). At the iteration $J + 2$ the perturbation is switched off and the relaxation continues. If the equilibrium configuration is stable, the perturbed solution relaxes to the axisymmetric solution; if not, it relaxes to the triaxial equilibrium configuration. In such a way, it is possible to find the critical value of γ , $T/|W|$, etc...

2.6. Extension to general relativity

The analysis of the triaxial instability of rotating stars has been recently extended to general relativity [33] in the case of *rigid* rotation. This latter assumption, crucial for finding a first integral of motion for non-axisymmetric relativistic configurations by following the procedure of Carter [34], corresponds physically to the viscosity driven instability, but not to the CFS instability. The translation of the technique presented in § 2.5 from the Newtonian framework to the general relativistic framework is not completely straightforward. Before considering the relativistic analysis let us consider again the Newtonian description of triaxial configurations.

2.6.1. Analysis of Newtonian triaxial configurations

Let us first come back to the problem of finding axisymmetric stationary solutions of rigidly rotating stars in Newtonian theory. In this theory two approaches are possible: The first one consists in finding an *equilibrium* configuration in a *non-Galilean* rotating frame (cf. § 2.5). In this frame the velocity vanishes and the term $\Omega^2 \rho$ in Eq. (8) is the apparent acceleration (centrifugal acceleration).

In the second approach (Galilean approach), the chosen reference frame is Galilean, the velocity of the fluid $v_{(\phi)} = \Omega \rho$ is not zero, and the term $\Omega \rho^2$ is due to the term $v^k \nabla_k v^i$ of the Euler equation (inertial acceleration). In both

approaches the problem consists in finding a steady-state solution. Note that the mass conservation equation

$$\partial n/\partial t + \nabla_i(nv^i) = 0 \quad (13)$$

is identically satisfied and that the equation (12) for the gravitational potential U is the same one in the two approaches.

The situation is different when looking for triaxial solutions. In fact for a Jacobi-like configuration, a steady state (equilibrium) solution exists only in the rotating frame. The questions that naturally arise are the following ones: is it possible to find an equivalent “equilibrium” configuration in a Galilean frame ? How to solve the Euler equation ? In order to answer these questions consider the unchanged Poisson equation (12) and the Euler and mass conservation equations ($x^1 = \rho, x^2 = z, x^3 = \phi$)

$$\partial v_i/\partial t + v^k \nabla_k v_i + \partial H(\rho, z, \phi, t)/\partial x^i + \partial U(\rho, z, \phi, t)/\partial x^i = 0 \quad (14)$$

$$\partial n(\rho, z, \phi, t)/\partial t + v^k \partial n(\rho, z, \phi, t)/\partial x^k + n \nabla_k v^k = 0 \quad (15)$$

altogether with the Poisson equation (12) for the potential which is unchanged. Let us look for a solution corresponding to a triaxial star undergoing rigid rotation about the z axis: $v_{(\rho)} = 0, v_{(z)} = 0, v_{(\phi)} = \Omega \rho$. The equations for the velocity read:

$$-\Omega^2 \rho + \partial H(\rho, z, \phi, t)/\partial \rho + \partial U(\rho, z, \phi, t)/\partial \rho = 0 \quad (16)$$

$$\partial H(\rho, z, \phi, t)/\partial z + \partial U(\rho, z, \phi, t)/\partial z = 0 \quad (17)$$

$$\partial H(\rho, z, \phi, t)/\partial \phi + \partial U(\rho, z, \phi, t)/\partial \phi = 0, \quad (18)$$

whereas Eq. (15) reduces to

$$\partial n(\rho, z, \phi, t)/\partial t + \Omega \partial n(\rho, z, \phi, t)/\partial \phi = 0 \quad (19)$$

It is easy to see that Eqs. (16)-(18) are satisfied if $H(\rho, z, \phi, t) + U(\rho, z, \phi, t) - 1/2 \Omega^2 \rho^2 = C(t)$, where $C(t)$ is an arbitrary function of t . This relation is a first integral of motion, very similar to relation (11).

The continuity equation (19) can be satisfied if we take $C(t) = \text{const}$ and consider n, H , and U as functions of the new variables (ρ, z, ψ) where

$$\psi := \phi - \Omega t. \quad (20)$$

Eq. (19) then becomes $-\Omega \partial n/\partial \psi + \Omega \partial n/\partial \phi = 0$, i.e. is identically satisfied.

From a geometrical point of view, we may say that the Newtonian spacetime of a rotating triaxial star has a one-parameter symmetry group, whose trajectories (orbits) are defined by $\psi = \text{const}$. The spacetime vectors that generate this symmetry group are called *Killing vectors*. In the frame associated with a Killing vector, the star appears in a steady state. The use of the notion of symmetry group or Killing vector fields allows the absolute definition (independent of any reference frame) of a steady state configuration. This is the definition that is going to be used in general relativity.

2.6.2. Rigid motion in general relativity

Before the symmetry breaking, the spacetime generated by the rotating star can be considered as *stationary* and *axisymmetric*, which means that there exist two Killing vector fields, k^α and m^α , such that k^α is timelike (at least far from the star) and m^α is spacelike and its orbits are closed curves. Moreover, in the case of rigid rotation, the spacetime is *circular*, which means that the 2-spaces orthogonal to both k^α and m^α are integrable in global 2-surfaces [37]. This latter property considerably simplifies the study of rotating stars because some global coordinates (t, r, θ, ϕ) may be chosen so that the metric tensor components exhibit only one non-vanishing off-diagonal term ($g_{t\phi}$). t and ϕ are coordinates associated with respectively the Killing vectors k^α and m^α : $k^\alpha = \partial/\partial t$ and $m^\alpha = \partial/\partial\phi$. The remaining coordinates (r, θ) span the 2-surfaces orthogonal to both k^α and m^α . In all numerical work on rotating stars to date (see e.g. ref. [35] for a review) *isotropic coordinates* are chosen, for which the two-dimensional line element differs from the flat space one by a conformal factor A^2 . In these coordinates, the components of the metric tensor are given by

$$g_{\alpha\beta} dx^\alpha dx^\beta = -N^2 dt^2 + B^2 r^2 \sin^2 \theta (d\phi - N^\phi dt)^2 + A^2 [dr^2 + r^2 d\theta^2] , \quad (21)$$

where the four functions N , N^ϕ , A and B depend on the coordinates (r, θ) only, the coordinates (t, ϕ) being associated with the Killing vector fields.

When the axisymmetry of the star is broken, the stationarity of spacetime is also broken. As discussed above, in the Newtonian theory, there is no inertial (Galilean) frame in which a rotating triaxial object appears stationary, i.e. does not depend upon the time. It can be stationary only in a corotating frame, which is not inertial, so that the stationarity is broken in this sense. In the general relativistic case, where the notion of a global inertial frame is in general meaningless, a rotating triaxial system is not stationary for it radiates away gravitational waves. Even if a corotating frame could be defined, the body could not be in a steady state in this frame, because it loses energy and angular momentum via gravitational radiation.

However, at the very point of the symmetry breaking, no gravitational wave has been emitted yet. As an approximation we neglect any subsequent gravitational radiation. Then, for a rigid rotation, there exists one Killing vector field l^α , which is proportional to the fluid 4-velocity u^α , hence

$$u^\alpha = \lambda l^\alpha , \quad (22)$$

where λ is a strictly positive scalar function. Equation (22) is the definition of a *rigid motion* according to Carter [34] ⁽²⁾ (i) there exists a Killing vector field;

⁽²⁾ More generally the relativistic concept of *rigidity* is defined by the requirement that the *expansion tensor* [cf. Eq. (A6) below] associated with the vector field u^α should vanish; it is easy to show that this requirement is fulfilled if u^α takes the form (22).

(ii) the fluid 4-velocity is parallel to this Killing vector. In the axisymmetric and stationary case, the rigid motion corresponds to the constant angular velocity $\Omega := u^\phi/u^t$, the Killing vector entering equation (22) being then

$$l^\alpha = k^\alpha + \Omega m^\alpha , \quad (23)$$

where k^α and m^α are the two Killing vectors defined above. The constancy of Ω ensures that l^α is a Killing vector too. The proportionality constant λ of equation (22) is nothing else than the component u^t of the 4-velocity u^α , where t is the coordinate associated with the Killing vector k^α . Note that the Killing vector l^α is generally timelike close to the star and spacelike far from it (beyond the “light-cylinder”).

In the non-axisymmetric case, k^α and m^α can no longer be defined as Killing vectors. We make instead the assumption that there exist (i) a vector field k^α which is timelike at least far from the star, (ii) a vector field m^α , which commutes with k^α , is spacelike everywhere and whose field lines are closed curves, (iii) a constant Ω such that the vector l^α defined by the combination (23) is a Killing vector and (iv) the fluid 4-velocity u^α is parallel to l^α . These hypotheses are the geometric translation of the approximation of rigid rotation and negligible gravitational radiation. The commutativity of k^α and m^α ensures that a coordinate system (t, r, θ, ϕ) can be found such that $k^\alpha = \partial/\partial t$ and $m^\alpha = \partial/\partial\phi$.

2.7. First integral of fluid motion in general relativity

The purpose of this section is to show that in the framework of general relativity, there still exists a first integral for the fluid motion, this result being exact in the axisymmetric and stationary case, and being valid within the approximation of the existence of the Killing vector l^α in the 3-D case.

As detailed in ref. [33], the first integral can be found in an elegant geometrical way, using the *canonical form* of the equation of fluid dynamics introduced by Lichnerowicz [36] and Carter [34] and involving Cartan’s calculus on differential forms. However, in the present lecture, we follow a different approach, based on the formulation of relativistic hydrodynamics in an accelerated frame (Appendix A). In doing so, a parallel can be developed with the two points of view of Newtonian physics recalled in § 2.6.1 (that of a rotating observer and an inertial (Galilean) observer).

The rotating observer is the observer \mathcal{O}_F comoving with the fluid, whose 4-velocity is u^α . The relativistic generalization of the “fixed” inertial observer is chosen to be the Eulerian observer \mathcal{O}_E of the 3+1 formalism [38], whose 4-velocity is denoted by n^α .

2.7.1. The point of view of the comoving observer

Let us consider the Euler equation (A21) in the frame of the fluid observer \mathcal{O}_F . Using notations of Appendix A, one has in this case, $v^\alpha = u^\alpha$, $V^\alpha = 0$ and

$E = e$, so that Eq. (A21) reduces to

$$\frac{1}{e+p} \bar{\nabla}_\alpha p + a_\alpha = 0 , \quad (24)$$

with $a_\alpha = u^\mu \nabla_\mu u_\alpha$. Let us recall that $\bar{\nabla}_\alpha$ denotes the covariant derivative within the 3-dimensional plane orthogonal to \mathcal{O}_F worldlines. Using Eq. (22) and the Killing identity $\nabla_{(\alpha} l_{\beta)} = 0$, we get $a_\alpha = -\bar{\nabla}_\alpha \ln \lambda$. Eq. (24) then becomes

$$\frac{1}{e+p} \bar{\nabla}_\alpha p - \bar{\nabla}_\alpha \ln \lambda = 0 , \quad (25)$$

from which a first integral of motion is immediately obtained:

$$H - \ln \lambda = \text{const.} \quad (26)$$

where H is defined by

$$H := \int \frac{dp}{e+p} = \ln \left(\frac{e+p}{m_B n} \right) , \quad (27)$$

m_B being the mean baryon mass. The second equality in Eq. (27) is a consequence of the First Law of Thermodynamics at zero temperature. This definition of H constitutes a relativistic generalization of the specific enthalpy introduced by Eq. (10).

2.7.2. The point of view of the Eulerian observer

Let us now consider the Eulerian observer \mathcal{O}_E . His 4-velocity is

$$n^\alpha = \frac{1}{N} (k^\alpha + N^\alpha) , \quad (28)$$

where N is the so-called *lapse function* and N^α the *shift vector* [38]. In the present case, $N^\alpha = N^\phi m^\alpha$. Using notations of Appendix A, one has $v^\alpha = n^\alpha$, $\omega_{\alpha\beta} = 0$ (the world lines of \mathcal{O}_E are orthogonal to the hypersurfaces $t = \text{const}$)⁽³⁾, $\theta_{\alpha\beta} = -K_{\alpha\beta}$, where $K_{\alpha\beta}$ is the extrinsic curvature tensor of the hypersurfaces $t = \text{const}$. [38], $V^\alpha = N^{-1} (\Omega - N^\phi) m^\alpha = N^{-1} l^\alpha - n^\alpha$, $\Gamma = N u^t = N \lambda$. The Euler equation (A19) then becomes

$$\begin{aligned} n^\mu \nabla_\mu V^\alpha - a_\mu V^\mu n^\alpha + V^\mu \bar{\nabla}_\mu V^\alpha - K^\alpha_\mu V^\mu + (K_{\mu\nu} V^\mu V^\nu - a_\mu V^\mu) V^\alpha \\ + \frac{1}{E+p} (\bar{\nabla}^\alpha p + V^\alpha n^\mu \nabla_\mu p) + a^\alpha = 0 . \end{aligned} \quad (29)$$

After straightforward calculations, making use of the fact that l^α is a Killing vector, the various terms that appear in this equation can be expressed as

$$n^\mu \nabla_\mu V^\alpha = -\frac{1}{N} (n^\mu \nabla_\mu \ln N) l^\alpha - \frac{1}{N} K^\alpha_\mu l^\mu \quad (30)$$

⁽³⁾ the fact that the rotation 2-form of the Eulerian observer vanishes, explains why \mathcal{O}_E is sometimes called the *locally non-rotating observer* [39].

$$V^\mu \bar{\nabla}_\mu V^\alpha = -\Gamma^{-3} \bar{\nabla}^\alpha \Gamma + (\Gamma^{-2} - 1) \bar{\nabla}^\alpha \ln N + n^\mu \nabla_\mu \ln N V^\alpha + 2N^{-1} K^\alpha_\mu l^\mu + N^{-2} K_{\mu\nu} l^\mu l^\nu n^\alpha \quad (31)$$

$$a^\alpha = \bar{\nabla}^\alpha \ln N \quad (32)$$

$$K_{\mu\nu} V^\mu V^\nu = N^{-2} K_{\mu\nu} l^\mu l^\nu = -\Gamma^{-3} n^\mu \nabla_\mu \Gamma + (\Gamma^{-2} - 1) n^\mu \nabla_\mu \ln N \quad (33)$$

Accordingly, Eq. (29) becomes

$$\nabla_\alpha (H + \ln N - \ln \Gamma) + N^{-1} n^\mu \nabla_\mu (H + \ln N - \ln \Gamma) l_\alpha = 0. \quad (34)$$

Taking the scalar product with l^α and using the fact that l^α is a symmetry generator, leads to $n^\mu \nabla_\mu (H + \ln N - \ln \Gamma) = 0$. Introducing this latter relation in (34), we get

$$H + \ln N - \ln \Gamma = \text{const.} \quad (35)$$

This first integral of motion is exactly the same as that obtained in the co-moving frame [Eq. (26)] (remember that $\lambda = \Gamma/N$). In the Newtonian limit, $\ln N \rightarrow U$ and $\ln \Gamma \rightarrow \rho^2 \Omega^2/2$, so that Eq. (35) reduces to Eq. (11), as expected.

2.8. Gravitational field equations

Let us now say a few words about the equations for the gravitational field in the general relativistic case. For axisymmetric rotating stars, these equations are well known (see e.g. ref. [35]). As concerns the 3-D case and within the approximation made above (existence of the Killing vector l^α), a natural approach would be to use the Geroch formalism [40] which reduces the 4-dimensional Einstein equations to 3-dimensional equations by forming the quotient of spacetime by the trajectories of the Killing vector field. However in the present case, the Killing vector l^α is timelike inside the light cylinder and spacelike outside it. Consequently the second-order operators that appear in Geroch's formalism change from elliptic to hyperbolic type across the light cylinder. From the numerical point of view, we would rather have operators of a constant kind. For this reason, we do not consider Geroch formalism but instead the classical 3+1 formalism [38], i.e. the foliation of spacetime by spacelike hypersurfaces Σ_t . Within Σ_t , we choose coordinates (r, θ, ϕ) according to the prescription of § 2.6.2. Next we introduce the coordinate ψ as in Eq. (20) : $\psi := \phi - \Omega t$. All the metric coefficients are then functions of the three variables (r, θ, ψ) . In the equations of the 3+1 formalism (cf. § 3.2 of [38]) appear partial derivatives with respect to t, r, θ and ϕ . We replace them by partial derivatives with respect to r, θ and ψ according to the rule

$$\frac{\partial u}{\partial t} \longrightarrow -\Omega \frac{\partial u}{\partial \psi} \quad \frac{\partial u}{\partial \phi} \longrightarrow \frac{\partial u}{\partial \psi}. \quad (36)$$

We then obtain only 3-dimensional equations. Another simplification arises from considering only the dominant terms in the non-axisymmetric part of the

equations. We report to ref. [33] for further details. Let us simply mention that within our approximation, the triaxial metric tensor writes

$$g_{\alpha\beta} dx^\alpha dx^\beta = -N(r, \theta, \psi)^2 dt^2 + B(r, \theta, \psi)^2 r^2 \sin^2 \theta [d\phi - N^\phi(r, \theta) dt]^2 + A(r, \theta, \psi)^2 [dr^2 + r^2 d\theta^2]. \quad (37)$$

Note that the metric coefficients given by Eq. (37) are the components of the metric tensor with respect to the coordinates (t, r, θ, φ) and expressed as functions of the coordinates (r, θ, ψ) .

Within this approximation, the Einstein equations reduce to four elliptic equations, for the functions N , N^ϕ , AN and BN . In the Newtonian limit, the equation for N reduces to the Poisson equation (12).

2.9. Numerical results

The non-linear 3-D elliptic equations resulting from the formalism developed above are solved iteratively by means of a spectral method [35], [41]. The initial conditions are stationary axisymmetric configurations, constructed by a 2-D general relativistic numerical code [35], [42]. The initial lapse function N is perturbed by a non-axisymmetric $l = 2, m = \pm 2$ “bar” term, in the same way as the Newtonian gravitational potential in § 2.5. The stability is determined by examining the subsequent evolution.

2.9.1. Tests of the numerical code

As a test of the relativistic code, the same value of the critical adiabatic index as that found by James [21] (Eq. 7) has been obtained at the Newtonian limit. Also in the Newtonian regime, it has been verified that when the polytropic index γ increases, the ratio $T/|W|$ at which the triaxial instability occurs, tends to the classical value for incompressible fluids: $T/|W|_{\text{crit}}(\gamma = \infty) = 0.1375$ (cf. § 2.1), as shown in Fig. 2. Another test of the code consists in comparing results in the compressible polytropic case with previous numerical calculations, in the non-relativistic regime. Ipser & Managan [43] and Hachisu & Eriguchi [44] have obtained numerical models of Newtonian triaxial rotating polytropes, analogous to the Jacobi ellipsoids. They did not determine γ_{crit} ⁽⁴⁾ but performed calculations with fixed $\gamma \geq 2.66$. The location of the triaxial bifurcation point along a sequence of $\gamma = 3$ polytropes resulting from the relativistic code [33] used at the Newtonian limit has been compared with that obtained by the above authors. The agreement is better than 0.5% with the critical angular velocity of Hachisu & Eriguchi [44] and of the order of 2% with their critical value of $T/|W|$; with Ipser & Managan [43], the agreement is better than 0.5% on both quantities.

⁽⁴⁾ However, Ipser & Managan state that their results indicate that the critical adiabatic index lies somewhere in the range $2.22 \leq \gamma_{\text{crit}} \leq 2.28$

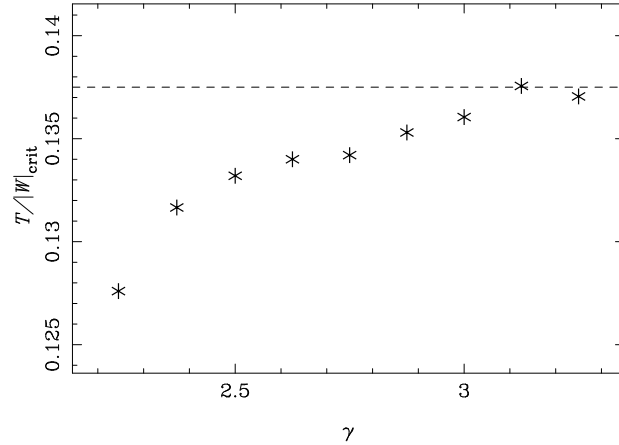


Fig. 2. — Ratio of the kinetic energy T to the gravitational potential energy W at the triaxial Jacobi-like bifurcation point along a sequence of rotating Newtonian polytropes, as a function of the adiabatic index γ . The dashed horizontal line corresponds to the theoretical value of $T/|W|$ for incompressible Maclaurin spheroids.

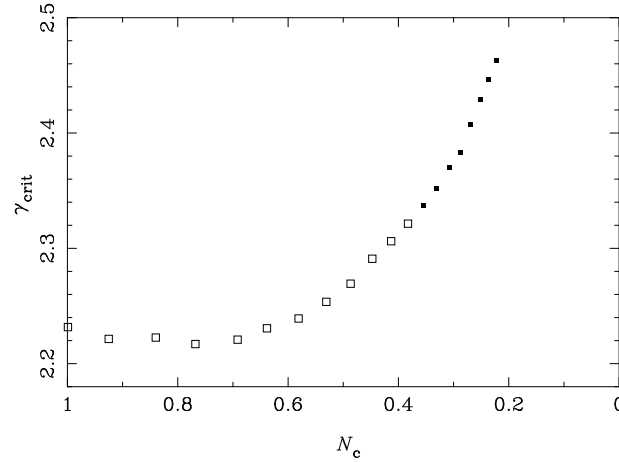


Fig. 3. — Critical polytropic index γ_{crit} as function of the lapse function N_c measured at the centre of the star. Black boxes indicate configurations unstable with respect to radial oscillations.

2.9.2. Results for polytropes

The investigation of relativistic polytropic stars is interesting in several respects. First, it represents a natural extension of former classical works restricted to the Newtonian case. Second, a polytropic EOS does not suffer from the thermodynamical inconsistency relative to tabulated EOS (cf. Sect. 4.2 of ref. [42]). It provides therefore an approximate but consistent model for real stars which allows a first investigation of relativistic effects. Since Newtonian polytropes obey a scaling law, γ_{crit} , the critical index for which the inset of the secular triaxial instability coincides with the maximum rotating case, is a global constant. In the relativistic case however, relativistic effects are supposed to influence the symmetry breaking and the critical index will depend on an appropriate parameter measuring the relativistic character of the object. A well suited quantity is the value N_c of the *lapse function* [38] at the centre of the star. We thus obtain a 2-dimensional parameter space for maximum rotating stars which is intersected by a curve representing the metastable configurations and thus separating the regions of stable and unstable stars respectively. Figure 3 shows the dependence of γ_{crit} on N_c ranging from the Newtonian to the extreme relativistic regime. In the moderately relativistic domain there appears a very slight decrease of γ_{crit} . The negative slope reveals that the inset of relativistic effects tends to destabilize the star (within the limitations imposed by the approximate character of the theoretical approach [33]), the maximum decrease of γ_{crit} being about 0.6 %. In the strong field region we observe a smooth growth of γ_{crit} beyond the maximum mass configurations due to the now persistently increasing stabilizing relativistic effects.

2.9.3. Results for realistic equations of state

We have determined in what condition the symmetry breaking may occur for rapidly rotating neutron stars built upon twelve EOS resulting from nuclear physics calculations. These “realistic” EOS are the same as those used in ref. [42] and we refer to this paper for a description of each EOS. The EOS are labeled by the following abbreviations: PandN refers to the pure neutron EOS of Pandharipande [45], BJI to model IH of Bethe & Johnson [46], FP to the EOS of Friedman & Pandharipande [47], HKP to the $n_0 = 0.17 \text{ fm}^{-3}$ model of Haensel et al. [48], DiazII to model II of Diaz Alonso [49], Glend1, Glend2 and Glend3 to respectively the case 1, 2, and 3 of Glendenning EOS [50], WFF1, WFF2 and WFF3 to respectively the AV₁₄ + UVII, UV₁₄ + UVII and UV₁₄ + TNI models of Wiringa et al. [51], and WGW to the $\Lambda_{\text{Bonn}}^{00}$ + HV model of Weber et al. [52].

Our results are shown in table I. For a given EOS, the axisymmetric rotating models form a two parameter family; each model can be labeled by its central energy density e_c and its (constant) angular velocity Ω . For a given value of e_c , Ω varies from zero to the Keplerian velocity Ω_K . Following the method described above, we have searched for a symmetry breaking of configurations rotating at the Keplerian velocity. For five EOS (Glend1, Glend3, DiazII, BJI

| EOS | M_{\max}^{stat} [M_{\odot}] | M_{\max}^{rot} [M_{\odot}] | P_K [ms] | P_{break} [ms] | $H_{c,\text{break}}$ | M_{break} [M_{\odot}] |
|--------|---|--|---------------|----------------------------|----------------------|---------------------------------------|
| HKP | 2.827 | 3.432 | 0.737 | 1.215 | 0.161 | 1.80 |
| WFF2 | 2.187 | 2.586 | 0.505 | 0.755 | 0.30 | 1.951 |
| WFF1 | 2.123 | 2.528 | 0.476 | 0.728 | 0.27 | 1.736 |
| WGW | 1.967 | 2.358 | 0.676 | | marginally stable | |
| Glend3 | 1.964 | 2.308 | 0.710 | | stable | |
| FP | 1.960 | 2.314 | 0.508 | 0.604 | 0.465 | 1.736 |
| DiazII | 1.928 | 2.256 | 0.673 | | stable | |
| BJI | 1.850 | 2.146 | 0.589 | | stable | |
| WFF3 | 1.836 | 2.172 | 0.550 | 0.714 | 0.325 | 1.909 |
| Glend1 | 1.803 | 2.125 | 0.726 | | stable | |
| Glend2 | 1.777 | 2.087 | 0.758 | | marginally stable | |
| PandN | 1.657 | 1.928 | 0.489 | | stable | |

Table I. — Neutron star properties according to various EOS: M_{\max}^{stat} is the maximum mass for static configurations, M_{\max}^{rot} is the maximum mass for rotating stationary configurations, P_K is the corresponding Keplerian period, P_{break} is the rotation period below which the symmetry breaking occurs, $H_{c,\text{break}}$ is the central log-enthalpy at the bifurcation point and M_{break} is the corresponding gravitational mass. The EOS are ordered by decreasing values of M_{\max}^{stat} .

and PandN), no symmetry breaking was found, whatever the value of Ω_K . These EOS are listed as “stable” in table I. For two EOS (WGW and Glend2) the evolution was not conclusive. These EOS are listed as “marginally stable” in table I. A better numerical precision could lead to a definitive conclusion. For five EOS (HKP, FP, WFF1, WFF2 and WFF3), the bar mode reveals to be unstable for some Keplerian velocities. Table I gives the period P_{break} , gravitational mass M_{break} and central log-enthalpy $H_{c,\text{break}}$ (cf. Eq. (27)) of the configuration having the lowest angular velocity and for which the symmetry breaking occurs.

3. CW EMISSION FROM PULSARS

As stated in the introduction, rapidly rotating neutron stars (pulsars) might be an important source of continuous gravitational waves. Moreover, the expected gravitational frequency is related to the rotation frequency and lies in the frequency bandwidth of the forthcoming LIGO and VIRGO interferometric detectors. While § 2 considers strong asymmetries resulting from an instability, we here investigate permanent slight asymmetries and the resulting continuous wave (CW) emission.

Various kinds of pulsar asymmetries have been suggested in the literature: first the crust of a neutron star is solid, so that its shape may not necessarily be

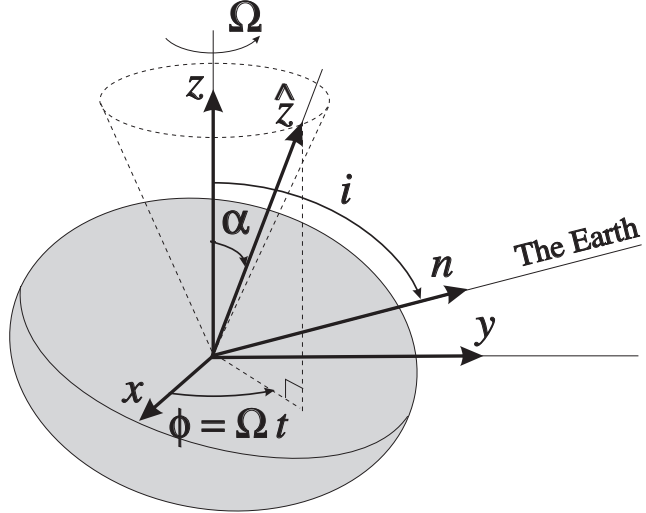


Fig. 4. — Geometry of the distorted neutron star.

axisymmetric under the effect of rotation, as it would be for a fluid: deviations from axisymmetry are supported by anisotropic stresses in the solid. The shape of the crust does not depend only on the early history of the neutron star, especially on the phase of crystallization of the crust[2], but also on star quakes. Due to its violent formation (supernova) or due to its environment (accretion disk), the rotation axis may not coincide with a principal axis of the neutron star moment of inertia and the star may precess. Even if it keeps a perfectly axisymmetric shape, a freely precessing body radiates gravitational waves. This effect is discussed in P.Haensel's lecture [2]. We consider another source of asymmetry here, linked to the magnetic field. Indeed, neutron stars are known to have important magnetic fields and the magnetic pressure (Lorentz forces exerted on the conducting matter) can distort the star if the magnetic axis is not aligned with the rotation axis, which is widely supposed to occur in order to explain the pulsar phenomenon.

3.1. Generation of gravitational waves by a rotating star

Let us consider a neutron star rotating at the angular velocity Ω about some axis (cf. Fig. 4). In the framework of general relativity, the mass quadrupole moment relevant for gravitational radiation is Thorne's quadrupole moment \mathcal{I}_{ij} [53]. Ipser [54] has shown that the leading term in the gravitational radiation field h_{ij} is given by a formula which is structurally identical to the quadrupole formula for Newtonian sources (cf. § 2.2 of L. Blanchet's lecture [1]), the Newtonian quadrupole being simply replaced by Thorne's quadrupole.

The non-axisymmetric deformation of neutron stars being very tiny, the total Thorne's quadrupole can be linearly decomposed into the sum of two pieces: $\mathcal{I}_{ij} = \mathcal{I}_{ij}^{\text{rot}} + \mathcal{I}_{ij}^{\text{dist}}$, where $\mathcal{I}_{ij}^{\text{rot}}$ is the quadrupole moment due to rotation ($\mathcal{I}_{ij}^{\text{rot}} = 0$ if the configuration is static) and $\mathcal{I}_{ij}^{\text{dist}}$ is the quadrupole moment due to the process that distorts the star, for example an internal magnetic field or anisotropic stresses from the nuclear interactions. Let us make the assumption that the distorting process has a privileged direction, i.e. that two of the three eigenvalues of $\mathcal{I}_{ij}^{\text{dist}}$ are equal. Let then α be the angle between the rotation axis and the principal axis of $\mathcal{I}_{ij}^{\text{dist}}$ which corresponds to the eigenvalue which is not degenerate (cf. Fig. 4). The two modes h_+ and h_\times of the gravitational radiation field in a transverse traceless gauge are then given by [55]

$$\begin{aligned} h_+ &= h_0 \sin \alpha \left[\frac{1}{2} \cos \alpha \sin i \cos i \cos \Omega(t - t_0) \right. \\ &\quad \left. - \sin \alpha \frac{1 + \cos^2 i}{2} \cos 2\Omega(t - t_0) \right] \end{aligned} \quad (38)$$

$$\begin{aligned} h_\times &= h_0 \sin \alpha \left[\frac{1}{2} \cos \alpha \sin i \sin \Omega(t - t_0) \right. \\ &\quad \left. - \sin \alpha \cos i \sin 2\Omega(t - t_0) \right], \end{aligned} \quad (39)$$

where i is the inclination angle of the “line of sight” with respect to the rotation axis (see Fig. 4) and

$$h_0 = \frac{16\pi^2 G}{c^4} \frac{I \epsilon}{P^2 r}, \quad (40)$$

where r is the distance of the star, $P = 2\pi/\Omega$ is the rotation period of the star, I its moment of inertia with respect of the rotation axis and $\epsilon := -3/2\mathcal{I}_{\hat{z}\hat{z}}^{\text{dist}}/I$ the *ellipticity* resulting from the distortion process.

From the formulae (38)-(39), it is clear that there is no gravitational emission if the distortion axis is aligned with the rotation axis ($\alpha = 0$ or π). If both axes are perpendicular ($\alpha = \pi/2$), the gravitational emission is monochromatic at twice the rotation frequency. In the general case ($0 < |\alpha| < \pi/2$), it contains two frequencies: Ω and 2Ω . For small values of α the emission at Ω is dominant. Replacing the physical constants by their numerical values results in the following expression for the gravitational wave amplitude [Eq. (40)]

$$h_0 = 4.21 \times 10^{-24} \left[\frac{\text{ms}}{P} \right]^2 \left[\frac{\text{kpc}}{r} \right] \left[\frac{I}{10^{38} \text{ kg m}^2} \right] \left[\frac{\epsilon}{10^{-6}} \right]. \quad (41)$$

Note that $I = 10^{38} \text{ kg m}^2$ is a representative value for the moment of inertia of a $1.4 M_\odot$ neutron star (see Fig. 12 of ref. [56]).

For the Crab pulsar, $P = 33$ ms and $r = 2$ kpc, so that Eq. (41) becomes

$$h_0^{\text{Crab}} = 1.89 \times 10^{-27} \left[\frac{I}{10^{38} \text{ kg m}^2} \right] \left[\frac{\epsilon}{10^{-6}} \right]. \quad (42)$$

For the Vela pulsar, $P = 89$ ms and $r = 0.5$ kpc, hence

$$h_0^{\text{Vela}} = 1.06 \times 10^{-27} \left[\frac{I}{10^{38} \text{ kg m}^2} \right] \left[\frac{\epsilon}{10^{-6}} \right]. \quad (43)$$

For the millisecond pulsar⁽⁵⁾ PSR 1957+20, $P = 1.61$ ms and $r = 1.5$ kpc, hence

$$h_0^{1957+20} = 1.08 \times 10^{-24} \left[\frac{I}{10^{38} \text{ kg m}^2} \right] \left[\frac{\epsilon}{10^{-6}} \right]. \quad (44)$$

At first glance, PSR 1957+20 seems to be a much more favorable candidate than the Crab or Vela. However, in the above formula, ϵ is in units of 10^{-6} and the very low value of the period derivative \dot{P} of PSR 1957+20 implies that its ϵ is at most 2×10^{-9} [2], [57]. Hence the maximum amplitude one can expect for this pulsar is $h_0^{1957+20} \sim 1.7 \times 10^{-27}$ and not 1.08×10^{-24} as Eq. (44) might suggest.

3.2. The specific case of magnetic field induced deformation

Let us assume that the distortion of the star is due to its own magnetic field. It is then expected that the ellipticity ϵ is proportional to the square of the *magnetic dipole moment* \mathcal{M} of the neutron star [55]:

$$\epsilon = \beta \frac{\mu_0}{4\pi G} \frac{R^2}{I^2} \mathcal{M}^2. \quad (45)$$

In this formula, R is the circumferential equatorial radius of the star and β is a dimensionless coefficient which measures the efficiency of this magnetic structure in distorting the star. In the following, we shall call β the *magnetic distortion factor*. Provided the magnetic field amplitude does not take (unrealistic) huge values ($> 10^{14}$ T), the formula (45) is certainly true, even if the magnetic field structure is quite complicated, depending on the assumed electromagnetic properties of the fluid: normal conductor, superconductor, ferromagnetic...

Now the observed spin down of radio pulsars is very certainly due to the low frequency magnetic dipole radiation. \mathcal{M} is then linked to the observed pulsar period P and period derivative \dot{P} by (cf e.g. Eq. (6.10.26) of ref. [58])

$$\mathcal{M}^2 = \frac{4\pi}{\mu_0} \frac{3c^3}{8\pi^2} \frac{IP\dot{P}}{\sin^2 \alpha}, \quad (46)$$

where α is the angle between the magnetic dipole moment \mathcal{M} and the rotation axis. For highly relativistic configurations, the vector \mathcal{M} is defined in the

⁽⁵⁾ We do not consider the “historical” millisecond pulsar PSR 1937+21 for it is more than twice farther away.

weak-field near zone (cf. Sect. 2.5 of ref. [59]), so is α . Inserting Eqs. (45) and (46) into Eq. (40) leads to the gravitational wave amplitude

$$h_0 = 6\beta \frac{R^2 \dot{P}}{crP \sin^2 \alpha}, \quad (47)$$

which can be cast in a numerically convenient form:

$$h_0 = 6.48 \times 10^{-30} \frac{\beta}{\sin^2 \alpha} \left[\frac{R}{10 \text{ km}} \right]^2 \left[\frac{\text{kpc}}{r} \right] \left[\frac{\text{ms}}{P} \right] \left[\frac{\dot{P}}{10^{-13}} \right]. \quad (48)$$

Among the 706 pulsars of the catalog by Taylor et al. [60], [61], the highest value of h_0 at fixed α , β and R , as given by Eq. (48), is achieved by the Crab pulsar ($P = 33$ ms, $\dot{P} = 4.21 \times 10^{-13}$, $r = 2$ kpc), followed by Vela ($P = 89$ ms, $\dot{P} = 1.25 \times 10^{-13}$, $r = 0.5$ kpc) and PSR 1509-58 ($P = 151$ ms, $\dot{P} = 1.54 \times 10^{-12}$, $r = 4.4$ kpc):

$$h_0^{\text{Crab}} = 4.08 \times 10^{-31} \left[\frac{R}{10 \text{ km}} \right]^2 \frac{\beta}{\sin^2 \alpha} \quad (49)$$

$$h_0^{\text{Vela}} = 1.81 \times 10^{-31} \left[\frac{R}{10 \text{ km}} \right]^2 \frac{\beta}{\sin^2 \alpha} \quad (50)$$

$$h_0^{\text{1509-58}} = 1.50 \times 10^{-31} \left[\frac{R}{10 \text{ km}} \right]^2 \frac{\beta}{\sin^2 \alpha} \quad (51)$$

$$h_0^{\text{1957+20}} = 4.51 \times 10^{-37} \left[\frac{R}{10 \text{ km}} \right]^2 \frac{\beta}{\sin^2 \alpha}. \quad (52)$$

We have added the millisecond pulsar PSR 1957+20 ($P = 1.61$ ms, $\dot{P} = 1.68 \times 10^{-20}$, $r = 1.5$ kpc) considered in § 3.1 to the list. From the above values, it appears that PSR 1957+20 is not a good candidate. This is not surprising since it has a small magnetic field (yielding a low \dot{P}). Even for the Crab and Vela pulsars, which have a large \dot{P} , the h_0 values as given by Eqs. (49), (50) are, at first glance, not very encouraging. Let us recall that with the $10^{-22} \text{ Hz}^{-1/2}$ expected sensitivity of the VIRGO experiment at a frequency of 30 Hz [62], [63], the minimal amplitude detectable within three years of integration is

$$h_{\min} \sim 10^{-26}. \quad (53)$$

Comparing this number with Eqs. (49)-(50), one realizes that in order to lead to a detectable signal, the angle α must be small and/or the distortion factor β must be large. In the former case, the emission occurs mainly at the frequency Ω . From Eq. (47) the gravitational wave amplitude can even be arbitrary large if $\alpha \rightarrow 0$. However, if α is too small, let say $\alpha < 10^{-2}$, the simple magnetic braking formula (46) certainly breaks down. So one cannot rely on a tiny α to yield a detectable amplitude. The alternative solution is to have a large β . For a Newtonian incompressible fluid with a uniform magnetic field, $\beta = 1/5$ [55]. In the following section, we give the β coefficients computed for more realistic models (compressible fluid, realistic equation of state, general relativity taken into account) with various magnetic field distributions.

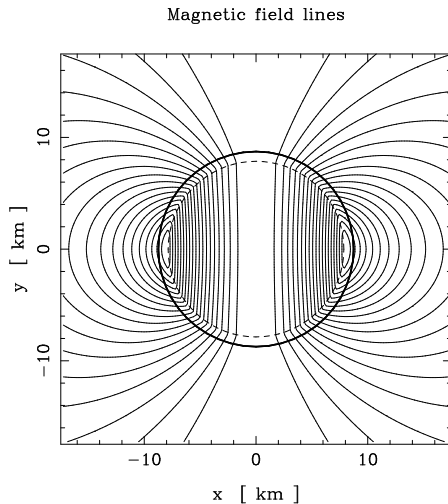


Fig. 5. — Magnetic field lines generated by a current distribution localized in the crust of the star. The thick line denotes the star's surface and the dashed line the internal limit of the electric current distribution. The distortion factor corresponding to this situation is $\beta = 8.84$.

3.3. Numerical results

We have developed a numerical code to compute the deformation of magnetized neutron stars within general relativity [55]. This code is an extension of that presented in ref. [59]. We report to this latter reference for details about the relativistic formulation of Maxwell equations and the technique to solve them. Let us simply recall here that the solutions obtained are fully relativistic and self-consistent, all the effects of the electromagnetic field on the star's equilibrium (Lorentz force, spacetime curvature generated by the electromagnetic stress-energy) being taken into account. The magnetic field is axisymmetric and poloidal. The numerical technique is based on a spectral method [41], [35].

The reference (non-magnetized) configuration is taken to be a $1.4 M_{\odot}$ static neutron star built with the equation of state UV₁₄ + TNI of Wiringa, Fiks & Fabrocini [51]. This latter is a modern, medium stiff equation of state. The circumferential radius is $R = 10.92$ km, the baryon mass $1.56 M_{\odot}$, the moment of inertia $I = 1.23 \times 10^{38}$ kg m² and the central value of g_{00} is 0.36, which shows that such an object is highly relativistic. Various magnetic field configurations have been considered; the most representative of them are presented hereafter.

Let us first consider the case of a perfectly conducting interior (normal matter, non-superconducting). The simplest magnetic configuration compatible with the MHD equilibrium of the star (cf. ref [59]) results in electric currents

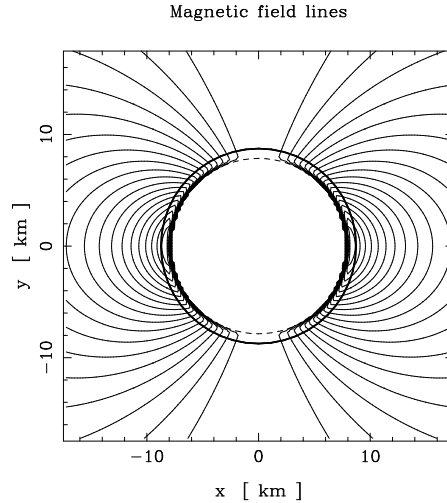


Fig. 6. — Magnetic field lines generated by a current distribution exterior to a type I superconducting core. The thick line denotes the star's surface and the dashed line the external limit of the superconducting region. The distortion factor corresponding to this situation is $\beta = 157$.

in the whole star with a maximum value at half the stellar radius in the equatorial plane. The computed distortion factor is $\beta = 1.01$, which is above the $1/5$ value of the uniform magnetic field/incompressible fluid Newtonian model [55] but still very low.

Another situation corresponds to electric currents localized in the neutron star crust only. Figure 5 presents one such configuration: the electric current is limited to the zone $r > r_* = 0.9 r_{\text{eq}}$. The resulting distortion factor is $\beta = 8.84$.

In the case of a superconducting interior, of type I, which means that all magnetic field has been expelled from the superconducting region, the distortion factor somewhat increases. In the configuration depicted in Fig. 6, the neutron star interior is superconducting up to $r_* = 0.9 r_{\text{eq}}$. For $r > r_*$, the matter is assumed to be a perfect conductor carrying some electric current. The resulting distortion factor is $\beta = 157$. For $r_* = 0.95 r_{\text{eq}}$, β is even higher: $\beta = 517$.

The above values of β , of the order $10^2 - 10^3$, though much higher than in the simple normal case, are still too low to lead to an amplitude detectable by the first generation of interferometric detectors in the case of the Crab or Vela pulsar [cf. Eqs. (49), (50) and (53)]. It is clear that the more disordered the magnetic field the higher β , the extreme situation being reached by a stochastic magnetic field: the total magnetic dipole moment \mathcal{M} almost vanishes, in agreement with the observed small value of \dot{P} , whereas the mean value of B^2

throughout the star is huge. Note that, according to Thompson & Duncan [64], turbulent dynamo amplification driven by convection in the newly-born neutron star may generate small scale magnetic fields as strong as 3×10^{11} T with low values of B_{dipole} outside the star and hence a large β .

In order to mimic such a stochastic magnetic field, we have considered the case of counter-rotating electric currents. The resulting distortion factor can be as high as $\beta = 5.7 \times 10^3$.

If the neutron star interior forms a type II superconductor, the magnetic field inside the star is organized in an array of quantized magnetic flux tubes, each tube containing a magnetic field $B_c \sim 10^{11}$ T [65]. As discussed by Ruderman [65], the crustal stresses induced by the pinning of the magnetic flux tubes is of the order $B_c B / 2\mu_0$, where B is the mean value of the magnetic field in the crust ($B \sim 10^8$ T for typical pulsars). This means that the crust is submitted to stresses $\sim 10^3$ higher than in the uniformly distributed magnetic field (compare $B_c B / 2\mu_0$ with $B^2 / 2\mu_0$). The magnetic distortion factor β should increase in the same proportion. We have not done any numerical computation to confirm this but plan to study type II superconducting interiors in a future work.

4. DISCUSSION AND CONCLUSION

4.1. Spontaneous symmetry breaking

From the results presented in Table I, it appears that only neutron stars whose mass is larger than $1.74 M_\odot$ meet the conditions of spontaneous symmetry breaking via the viscosity-driven instability. The above minimum mass is much lower than the maximum mass of a fast rotating neutron star for a stiff EOS ($3.2 M_\odot$ [42]). Note that the critical period at which the instability happens ($P = 1.2$ ms) is not far from the lowest observed one (1.56 ms). The question that naturally arises is : do these heavy neutron stars exist in nature ? Only observations can give the answer; in fact, the numerical modelling of a supernova core and its collapse [66] cannot yet provide us with a reliable answer. The masses of 17 neutron stars (all in binary systems) are known [67]. Among them, four masses (all in binary radio pulsars) are known with a precision better than 10% and they turn out to be around $1.4 M_\odot$ (see Table III in A. Wolszczan's lecture [68]). Among the X-ray binary neutron stars, two of them seem to have a higher mass: 4U 1700-37 and Vela X-1 ($1.8 \pm 0.5 M_\odot$ and $1.8 \pm 0.3 M_\odot$ respectively). These objects show that neutron stars in binary systems may have a mass larger than $1.7 M_\odot$.

A natural question that may arise is: why do X-ray binary neutron stars, which are believed to be the progenitors of binary radio pulsars, would have a mass larger than the latter ones ? We have not yet any reliable answer to this question. A first (pessimistic) answer is that the measurements of X-ray neutron star masses are not as reliable (compare the error bars of the masses of the binary radio pulsars with the ones of the X-ray binaries in Fig. 3 of

ref. [67]). Actually it should be noticed that the error bars of the X-ray pulsars do not have the same statistical meaning as the error bars of the binary radio pulsars [69]: they give only the extremum limits of neutron star masses in the X-ray binary. Consequently $1.4 M_{\odot}$ is not incompatible with these masses. If this is really the case forget all we have said about the above instability mechanisms: only the CFS mechanism for $m > 2$ can work, provided that the viscosity is low enough, which does not seem to be the case (especially if the “mutual friction” in the superfluid interior is taken into account [28]).

A related question arises naturally: why are the observed masses of millisecond radio pulsars almost identical? Following the standard model, a millisecond radio pulsar is a recycled neutron star, spun up by the accretion of mass and angular momentum from a companion. The observed mass and angular velocity are those of the end of the accretion process. Consequently the accreted mass depends on the history of the system and on the nature of the companion. By supposing “per absurdo” that all neutron stars are born with the same mass, it is difficult to understand why the accreted mass is the *same* for all neutron stars. A possible answer is that this could result from some observational selection effect. For example, suppose that accreted matter quenches the magnetic field, it is then easy to imagine that the final external magnetic field depends on the mass of the accreted plasma. If the accreted mass is large enough, the magnetic field can be lower than the critical value for which the pulsar mechanism works. On the contrary, if the accreted mass is quite small, the magnetic field is large and the life time of the radio pulsar phase is shorter and consequently more difficult to observe.

Let us conclude by saying that a lot of questions are still open about these systems. If we knew everything about neutron stars, such an observation would be a waste of time. The only thing that we can recommend is to stay open minded.

4.2. CW emission from pulsars

In this lecture, we have also investigated the CW emission resulting from the magnetic field induced distortion of neutron stars. The computations presented in § 3.3 show that the distortion at fixed magnetic dipole moment depends very sensitively on the magnetic configuration. The case of a perfect conductor interior with toroidal electric currents is the less favorable one, even if the currents are concentrated in the crust. Stochastic magnetic fields (that we modeled by considering counter-rotating currents) enhance the deformation by several orders of magnitude and may lead to a detectable amplitude for a pulsar like the Crab. As concerns superconducting interiors — the most realistic configuration for neutron stars — we have studied type I superconductors numerically, with a simple magnetic structure outside the superconducting region. The distortion factor is then $\sim 10^2$ to 10^3 higher than in the normal (perfect conductor) case, but still insufficient to lead to a positive detection by the first generation of kilometric interferometric detectors. We have not studied in detail the

type II superconductor but have put forward some argument which makes it a promising candidate for gravitational wave detection.

Acknowledgments

We warmly thank Joachim Frieben and Paweł Haensel for their careful reading of the preliminary version of these notes.

Problem:

Show that, at fixed angular momentum, the kinetic energy of an incompressible fluid in a cylinder is minimal for rigid rotation.

Solution:

Let $\Omega(\rho, z)$ be the angular velocity ($\rho = \sqrt{x^2 + y^2}$). The kinetic energy of the fluid is given by $T = \int_V 1/2 n\Omega^2(\rho, z)\rho^2 dV$ where n is the density of the fluid (assumed to be constant). We have to find an extremum of this quantity under the constraint that the angular momentum $L = \int_V n\Omega(\rho, z)\rho^2 dV$ has a fixed value. By means of the Lagrangian multiplier technique, this amounts to find an extremum of

$$\int_V \frac{1}{2} n\Omega^2(\rho, z)\rho^2 dV + \lambda \int_V n\Omega(\rho, z)\rho^2 dV , \quad (54)$$

where λ is the Lagrangian multiplier. By performing the variation with respect to Ω we obtain

$$\int_V (\Omega(\rho, z)\rho^2 + \lambda\rho^2) \delta\Omega dV = 0 , \quad (55)$$

from which $\Omega = \text{const.}$

Appendix A

RELATIVISTIC HYDRODYNAMICS IN AN ACCELERATED FRAME

In this appendix, we examine how to re-write the equation of momentum-energy conservation

$$\nabla_\mu T^{\mu\alpha} = 0 \quad (A1)$$

as a system of evolution equations with respect to a given observer \mathcal{O} , the evolved variables being the energy density and the fluid velocity, both measured by \mathcal{O} . We consider perfect fluids only:

$$T^{\alpha\beta} = (e + p) u^\alpha u^\beta + p g^{\alpha\beta} , \quad (A2)$$

so that the equation for the fluid velocity will constitute a relativistic generalization of the *Euler equation* of classical hydrodynamics.

The observer \mathcal{O} is completely arbitrary; he is simply described by its 4-velocity v^α . Strictly speaking we consider a *family* of observers \mathcal{O} (a *congruence* of worldlines), so that v^α constitutes a smooth vector field on spacetime. A fundamental tensor field related to \mathcal{O} is the projection operator onto the 3-space P orthogonal to v^α :

$$q_{\alpha\beta} := g_{\alpha\beta} + v_\alpha v_\beta . \quad (\text{A3})$$

The 3-space P is made of spacelike vectors and can be thought as the “physical” three-dimensional space “felt” by the observer \mathcal{O} . Note that if \mathcal{O} is rotating ($\omega_{\alpha\beta} \neq 0$, see below), the vector space P is not integrable in global 3-surfaces.

The motion of the observer \mathcal{O} through spacetime is characterized by the Ehlers decomposition of $\nabla_\beta v_\alpha$ (see, e.g., Sect. 4.1 of ref. [70])

$$\nabla_\beta v_\alpha = \omega_{\alpha\beta} + \theta_{\alpha\beta} - a_\alpha v_\beta , \quad (\text{A4})$$

where

$$\omega_{\alpha\beta} := q_\alpha^\mu q_\beta^\nu \nabla_{[\nu} v_{\mu]} \quad (\text{A5})$$

is the *rotation 2-form* of \mathcal{O} ,

$$\theta_{\alpha\beta} := q_\alpha^\mu q_\beta^\nu \nabla_{(\nu} v_{\mu)} \quad (\text{A6})$$

is the *expansion tensor* of \mathcal{O} and

$$a_\alpha := v^\mu \nabla_\mu v_\alpha \quad (\text{A7})$$

is the *4-acceleration* of \mathcal{O} .

For a 4-vector W^α lying in the “physical space” P of \mathcal{O} ($v_\mu W^\mu = 0$), we introduce the *3-covariant derivative* with respect to \mathcal{O} as

$$\bar{\nabla}_\alpha W_\beta := q_\alpha^\mu q_\beta^\nu \nabla_\mu W_\nu . \quad (\text{A8})$$

This definition results in the following relation between the 4-covariant and the 3-covariant derivatives:

$$\nabla_\alpha W_\beta = \bar{\nabla}_\alpha W_\beta - v_\alpha v^\mu \nabla_\mu W_\beta + (\theta_{\alpha\mu} W^\mu - \omega_{\alpha\mu} W^\mu) v_\beta , \quad (\text{A9})$$

from which the following relation between the 4-divergence and the 3-divergence is immediately derived:

$$\nabla_\mu W^\mu = \bar{\nabla}_\mu W^\mu + a_\mu W^\mu . \quad (\text{A10})$$

The fluid motion as seen by the observer \mathcal{O} is specified by the *Lorentz factor*

$$\Gamma := -v_\mu u^\mu , \quad (\text{A11})$$

and the *3-velocity*

$$V^\alpha := \frac{1}{\Gamma} q^\alpha_\mu u^\mu . \quad (\text{A12})$$

V^α belongs to P and is the fluid velocity as measured by the observer \mathcal{O} with his clock and his ruler. The following relations are immediate consequences of the above definitions:

$$u^\alpha = \Gamma(V^\alpha + v^\alpha) \quad (\text{A13})$$

$$\Gamma = (1 - V_\mu V^\mu)^{-1/2}. \quad (\text{A14})$$

The fluid energy density as measured by \mathcal{O} is given by the formula

$$E = T_{\mu\nu} v^\mu v^\nu, \quad (\text{A15})$$

or, according to the form (A2) of $T_{\mu\nu}$,

$$E = \Gamma^2(e + p) - p. \quad (\text{A16})$$

From this expression, it is clear that the kinetic energy of the fluid with respect to \mathcal{O} is included in the energy density E via the Lorentz factor Γ .

Having set these definitions, let us now examine the equations of motion deduced from the momentum-energy conservation, Eq. (A1), which, using the perfect fluid form (A2) of $T_{\alpha\beta}$, can be written as

$$(e + p)u^\mu \nabla_\mu u^\alpha + \nabla_\mu [(e + p)u^\mu] u^\alpha + \nabla^\alpha p = 0 \quad (\text{A17})$$

The evolution equation for the fluid energy density E as measured by \mathcal{O} is obtained by projecting Eq. (A17) along v^α . Invoking Eqs. (A13) and (A16), one obtains after straightforward calculations

$$v^\mu \nabla_\mu E + \bar{\nabla}_\mu [(E + p)V^\mu] + (E + p)(2a_\mu V^\mu + \theta_\mu^\mu + \theta_{\mu\nu} V^\mu V^\nu) = 0. \quad (\text{A18})$$

The relativistic generalization of the Euler equation is obtained by projecting Eq. (A17) onto P , by means of $q_{\alpha\beta}$. After straightforward calculations (at a certain stage, use must be made of Eq. (A18)) one obtains

$$\begin{aligned} v^\mu \nabla_\mu V^\alpha - a_\mu V^\mu v^\alpha + V^\mu \bar{\nabla}_\mu V^\alpha + (\omega_\mu^\alpha + \theta_\mu^\alpha) V^\mu - (a_\mu V^\mu + \theta_{\mu\nu} V^\mu V^\nu) V^\alpha \\ = -\frac{1}{E + p} (\bar{\nabla}^\alpha p + V^\alpha v^\mu \nabla_\mu p) - a^\alpha. \end{aligned} \quad (\text{A19})$$

Note that the first two terms on the left-hand side, $v^\mu \nabla_\mu V^\alpha - a_\mu V^\mu v^\alpha$, constitute the *Fermi-Walker derivative* [70] of V^α with respect to v^α . The Fermi-Walker derivative measures the rate of change *within* P of V^α with respect to the proper time of \mathcal{O} . If the observer \mathcal{O} has set up a local coordinate system, with respect to which the length of the vectors in P are evaluated, a derivative operator more convenient than $v^\mu \nabla_\mu$ is the *Lie derivative* along v^α , \mathcal{L}_v . The term which naturally appears on the left-hand side of Eq. (A19) is then the *convected derivative* of V^α [71], [72] :

$$D_v V^\alpha := \mathcal{L}_v V^\alpha - a_\mu V^\mu v^\alpha = v^\mu \nabla_\mu V^\alpha - (\omega_\mu^\alpha + \theta_\mu^\alpha) V^\mu - a_\mu V^\mu v^\alpha. \quad (\text{A20})$$

The Euler equation (A19) then becomes

$$\begin{aligned} D_v V^\alpha + V^\mu \bar{\nabla}_\mu V^\alpha + 2(\omega^\alpha_\mu + \theta^\alpha_\mu) V^\mu - (a_\mu V^\mu + \theta_{\mu\nu} V^\mu V^\nu) V^\alpha \\ = -\frac{1}{E+p} (\bar{\nabla}^\alpha p + D_v p V^\alpha) - a^\alpha. \end{aligned} \quad (\text{A21})$$

In the Newtonian limit, D_v reduces simply to $\partial/\partial t$. Moreover, the $V^\mu \bar{\nabla}_\mu V^\alpha$ gives the classical term $(\vec{V} \cdot \vec{\nabla}) \vec{V}$ and $2\omega^\alpha_\mu V^\mu$ gives the Coriolis term $2\vec{\omega} \times \vec{V}$, induced by the rotation of the observer \mathcal{O} with respect to some inertial frame. The terms involving $\theta_{\alpha\beta}$ are due to the non-rigidity of the frame set up by the observer \mathcal{O} . On the right-hand side, the classical $(1/\rho) \vec{\nabla} p$ term is recognized, supplemented by the special relativistic term $(\partial p/\partial t) \vec{V}$. The last term, the acceleration $-a^\alpha$, contains gravitational as well as centrifugal forces.

References

- [1] Blanchet L., this volume.
- [2] Haensel P., this volume.
- [3] Chandrasekhar S., *Phys. Rev. Lett.* **24** (1970) 611.
- [4] Friedman J.L., Schutz B.F., *Astrophys. J.* **222** (1978) 281.
- [5] Friedman J.L., *Commun. Math. Phys.* **62** (1978) 247.
- [6] Roberts P.H., Stewartson K., *Astrophys. J.* **137** (1963) 777.
- [7] Chandrasekhar S., *Ellipsoidal figures of equilibrium* (Yale University Press, New Haven, 1969) p. 1.
- [8] Tassoul J.-L., *Theory of rotating stars* (Princeton University Press, Princeton, 1978) p. 1.
- [9] Christodoulou D.M., Contopoulos J., Kazanas D., Interchange method in incompressible magnetized Couette flow: structural and magnetorotational instabilities, preprint.
- [10] Lai D., Rasio F.A., Shapiro S.L., *Astrophys. J. Suppl.* **88** (1993) 205.
- [11] Press W.H., Teukolsky S.A., *Astrophys. J.* **181** (1973) 513.
- [12] Miller B.D., *Astrophys. J.* **187** (1974) 609.
- [13] Landau L.D., E. Lifchitz, *Physique statistique* (Mir, Moscow, 1984) p. 488.
- [14] Bertin G., Radicati L.A., *Astrophys. J.* **206** (1976) 815.
- [15] Christodoulou D.M., Kazanas D., Shlosman I., Tohline J.E., *Astrophys. J.* **446** (1995) 472.
- [16] Christodoulou D.M., Kazanas D., Shlosman I., Tohline J.E., *Astrophys. J.* **446** (1995) 485.
- [17] Christodoulou D.M., Kazanas D., Shlosman I., Tohline J.E., *Astrophys. J.* **446** (1995) 500.
- [18] Christodoulou D.M., Kazanas D., Shlosman I., Tohline J.E., *Astrophys. J.* **446** (1995) 510.
- [19] Jeans J.H., *Problems of cosmogony and stellar dynamics* (Cambridge University Press, Cambridge, 1919) p. 1.

- [20] Jeans J.H., *Astronomy and cosmogony* (Cambridge University Press, Cambridge, 1928) p. 1. Reprinted in 1961 (Dover, New York).
- [21] James R.A., *Astrophys. J.* **140** (1964) 552.
- [22] Ipser J.R., Managan R.A., *Astrophys. J.* **292** (1985) 517.
- [23] Managan R.A., *Astrophys. J.* **294** (1985) 463.
- [24] Imamura J.N., Friedman J.L., Durisen R.H., *Astrophys. J.* **294** (1985) 474.
- [25] Lindblom L., *Astrophys. J.* **438** (1995) 265.
- [26] Yoshida S., Eriguchi Y., *Astrophys. J.* **438** (1995) 830.
- [27] Friedman J.L., Ipser J.R., *Phil. Trans. R. Lond. A* **340** (1992) 391. Reprinted in: *Classical general relativity*, ed. S. Chandrasekhar (Oxford University Press, Oxford, 1993).
- [28] Lindblom L., Mendell G., *Astrophys. J.* **444** (1995) 804.
- [29] Ipser J.R., Managan R.A., *Astrophys. J.* **282** (1984) 287.
- [30] Wagoner R.W., *Astrophys. J.* **278** (1984) 345.
- [31] Lai D., Shapiro S.L., *Astrophys. J.* **442** (1995) 259.
- [32] Lindblom L., Detweiler S.L., *Astrophys. J.* **211** (1977) 565.
- [33] Bonazzola S., Frieben J., Gourgoulhon E., *Astrophys. J.* **460** (1996) 379.
- [34] Carter B., in *Active Galactic Nuclei*, eds. C. Hazard & S. Mitton (Cambridge University Press, Cambridge, 1979).
- [35] Bonazzola S., Gourgoulhon E., Salgado M., Marck J.-A., *Astron. Astrophys.* **278** (1993) 421.
- [36] Lichnerowicz A., *Relativistic hydrodynamics and magnetohydrodynamics* (W.A. Benjamin Inc., New York, 1967) p. 1.
- [37] Carter B., 1973, in *Black Holes — Les Houches 1972*, eds. C. DeWitt & B.S. DeWitt (Gordon & Breach, New York, 1973).
- [38] Abrahams A.M., York J.W., this volume.
- [39] Bardeen J.M., *Astrophys. J.* **162** (1970) 71.
- [40] Geroch R., *J. Math. Phys.* **12** (1971) 918.
- [41] Bonazzola S., Gourgoulhon E., Marck J.-A., this volume.
- [42] Salgado M., Bonazzola S., Gourgoulhon E., Haensel P., *Astron. Astrophys.* **291** (1994) 155.
- [43] Ipser J.R., Managan R.A., *Astrophys. J.* **250** (1981) 362.
- [44] Hachisu I., Eriguchi Y., *Prog. Theor. Phys.* **68** (1982) 206.
- [45] Pandharipande V.R., *Nucl. Phys. A* **174** (1971) 641.
- [46] Bethe H.A., Johnson M.B., *Nucl. Phys. A* **230** (1974) 1.
- [47] Friedman B., Pandharipande V.R., *Nucl. Phys. A* **361** (1981) 502.
- [48] Haensel P., Kutschera M., Prószyński M., *Astron. Astrophys.* **102** (1981) 299.
- [49] Diaz Alonso J., *Phys. Rev. D* **31** (1985) 1315.
- [50] Glendenning N.K., *Astrophys. J.* **293** (1985) 470.
- [51] Wiringa R.B., Fiks V., Fabrocini A., *Phys. Rev. C* **38** (1988) 1010.
- [52] Weber F., Glendenning N.K., Weigel M.K., *Astrophys. J.* **373** (1991) 579.
- [53] Thorne K.S., *Rev. Mod. Phys.* **52** (1980) 299.

- [54] Ipser J.R., *Astrophys. J.* **166** (1971) 175.
- [55] Bonazzola S., Gourgoulhon E., *Astron. Astrophys.*, in press (preprint: [astro-ph/9602107](http://arxiv.org/abs/astro-ph/9602107)).
- [56] Arnett W.D., Bowers R.L., *Astrophys. J. Suppl.* **33** (1977) 415.
- [57] New K.C.B., Chanmugam G., Johnson W.W., Tohline J.E., *Astrophys. J.* **450** (1995) 757.
- [58] Straumann N., General relativity and relativistic astrophysics (Springer Verlag, Berlin, 1984) p. 353.
- [59] Bocquet M., Bonazzola S., Gourgoulhon E., Novak J., *Astron. Astrophys.* **301** (1995) 757.
- [60] Taylor J.H., Manchester R.N., Lyne A.G., *Astrophys. J. Suppl.* **88** (1993) 529.
- [61] Taylor J.H., Manchester R.N., Lyne A.G., Camilo F., unpublished work (1995).
- [62] Brillet A., Giazotto A., this volume.
- [63] Bondu F., PhD Thesis (Université Paris XI, 1996).
- [64] Thompson C., Duncan R.C., *Astrophys. J.* **408** (1993) 194.
- [65] Ruderman M., *Astrophys. J.* **382** (1991) 576.
- [66] Müller E., this volume.
- [67] Thorsett S.E., Arzoumanian Z., McKinnon M.M., Taylor J.H., *Astrophys. J.* **405** (1993) L29.
- [68] Wolszczan A., this volume.
- [69] Lindblom L., private communication.
- [70] Hawking S.W., Ellis G.F.R., The large scale structure of space-time (Cambridge University Press, Cambridge, 1973) p. 1.
- [71] Carter B., Quintana H., *Proc. R. Soc. Lond. A* **331** (1972) 57.
- [72] Carter B., *Proc. R. Soc. Lond. A* **372** (1980) 169.